*Journal of Sound and Vibration* (2002) **256**(1), 65–79
doi:10.1006/jsvi.2001.4199, available online at http://www.idealibrary.com on IDEAL®

# DYNAMICS AND DISTRIBUTED CONTROL OF CONICAL SHELLS LAMINATED WITH FULL AND DIAGONAL ACTUATORS

H. S. Tzou, D. W. Wang and W. K. Chai

*Department of Mechanical Engineering, Structronics Lab., University of Kentucky, Lexington, KY* 40506-0108, *U.S.A. E-mail: hstzou@engr.uky.edu*

(*Received* 29 *January* 2001, *and in final form* 6 *December* 2001)

Nozzles, rocket fairings and many engineering structures/components are often made of conical shells. This paper focuses on the finite element modelling, analysis, and control of conical shells laminated with distributed actuators. Electromechanical constitutive equations and governing equations of a generic piezo(electric)elastic continuum are defined first, followed by the strain–displacement relations and electric field–potential relations of laminated shell composites. Finite element formulation of a piezoelastic shell element with non-constant Lamé parameters is briefly reviewed; element and system matrix equations of the piezoelastic shell sensor/actuator/structure laminate are derived. The system equation reveals the coupling of mechanical and electric fields, in which the electric force vector is often used in distributed control of shells. Finite element eigenvalue solutions of conical shells are compared with published numerical results first. Distributed control of the conical shell laminated with piezoelectric shell actuators is investigated and control effects of three actuator configurations are evaluated.



## 1. INTRODUCTION

Conical shell structures and components are often used as nozzles, injectors, rocket fairings, fan blades, etc., in aerospace structures and turbomachinery. Undesirable dynamic oscillations not only degrade the performance, but also influence structural integrity and reliability. Dynamics and vibrations of conical shells have been widely studied [1, 2]; however, distributed vibration control of conical shells has not caught much attention over the years. Recent rapid development of smart structures and structronic systems provides many new design options for the next-generation high-performance mechanical and structural systems [3, 4]. Based on the smart structures and structronics technology, this study is to evaluate dynamic characteristics and control effects of conical shells laminated with fully or diagonally distributed piezoelectric sensor/actuator layers.

Piezoelectrics, shape-memory materials, electrostrictive materials, magnetostrictive materials, photostrictive materials, electro- and magneto-rheological materials, etc., are electro-, magneto-, and/or optoelectro-mechanically *controllable* materials and thus they are generally accepted as "smart" materials [3, 4]. Among these smart materials, piezoelectric materials are probably the most popular smart materials applied to both sensor and actuator applications. Distributed sensing and control of shells and plates using piezoelectric materials have been investigated over the years [5]. Distributed control effects of one-dimensional and two-dimensional planar structures, e.g., beams and plates, are

0022-460X/02/$35.00 

studied and compared [5–11], and also rings and shells [5, 12–15]. Piezothermoelastic characteristics and temperature influences on piezoelectric sensors and actuators of beam-type precision devices and cylindrical shell structures have been studied [15–17]. This study is to investigate the modelling, analysis, and distributed vibration control of piezoelectric laminated conical shells. Fundamental piezoelectric constitutive and governing equations are briefly reviewed and the formulation of a new piezo(electric)-elastic triangle composite shell finite element with *non-constant* radii of curvature is presented. Dynamic characteristics and distributed vibration controls of conical shells are investigated. Control effects of three actuator designs are evaluated.

## 2. GOVERNING EQUATIONS

Electromechanical constitutive and equilibrium equations of a piezo(electric)elastic continuum are defined first, and followed by generic shell strain–displacement definitions of a double-curvature piezoelastic shell laminate in this section. Finite element formulations are presented in the next section. The linear piezoelectric constitutive equations coupling the electric and elastic fields are [5]

$$T_{ij} = c_{ijkl}^{E,\theta}(S_{kl} - S_{kl}^0) - e_{ijm}^{\theta} E_m \quad \text{and} \quad D_n = e_{nkl}^{\theta}(S_{kl} - S_{kl}^0) + \varepsilon_{nm}^{S,\theta} E_m, \tag{1, 2}$$

where $T_{ij}$ and $D_i$ denote the stress and electric displacements, $c_{ijkl}^{E,\theta}$, $e_{ijm}^{\theta}$, and $\varepsilon_{nm}^{S,\theta}$, respectively, denote the elastic moduli, piezoelectric coefficient, dielectric constants, $S_{kl}$, and $S_{kl}^0$ are the strain, and initial strains. In addition, the superscripts $E$, $\theta$, and $S$ denote the coefficients defined at a constant electric field, temperature and strain respectively. For a piezoelastic shell medium, with a volume $V$ and a limited surface area $S$, subjected to both electric and mechanical excitations, the linear governing equations, including the coupling among deformation and electric potential, can be defined as [16–18]

$$T_{ij,j} + f_{bi} = \rho \ddot{U}_i \quad \text{and} \quad D_{i,i} = 0, \tag{3, 4}$$

where $f_{bi}$, $\rho$, and $\ddot{U}_i$, respectively, denote the body force, mass density, and acceleration; and $U_i$ is the displacement. Note that Einstein's summation convention is used in the expressions.

A piezoelastic laminated shell continuum is composed of $N$ laminae, and each lamina can be either an elastic material or a piezoelectric material, Figure 1. It is assumed that the piezoelastic shell is exposed to mechanical and electrical inputs. Considering small deformation of the laminated piezoelastic shell, one can derive the strain $S_{ij}$ and electric field $E_i$ equations defined in an orthogonal curvilinear co-ordinate system $(\alpha_1, \alpha_2, \alpha_3)$. The strain $(S_{ij})$ – displacement relations and electric field $(E_i)$ – electric potential $(\phi)$ relations in a tri-orthogonal shell co-ordinate system are defined as [5, 17]

$$S_{11} = \frac{1}{(1 + \alpha_3/R_1)A_1}\left[\frac{\partial U_1}{\partial \alpha_1} + \frac{1}{A_2}\frac{\partial A_1}{\partial \alpha_2} U_2 + \frac{A_1}{R_1} U_3\right], \tag{5}$$

$$S_{22} = \frac{1}{(1 + \alpha_3/R_2)A_2}\left[\frac{\partial U_2}{\partial \alpha_2} + \frac{1}{A_1}\frac{\partial A_2}{\partial \alpha_1} U_1 + \frac{A_2}{R_2} U_3\right], \quad S_{33} = \frac{\partial U_3}{\partial \alpha_3}, \tag{6, 7}$$

$$S_{12} = \frac{1}{2(1 + \alpha_3/R_1)A_1}\left[\frac{\partial U_2}{\partial \alpha_1} - \frac{1}{A_2}\frac{\partial A_1}{\partial \alpha_2} U_1\right] + \frac{1}{2(1 + \alpha_3/R_2)A_2}\left[\frac{\partial U_1}{\partial \alpha_2} - \frac{1}{A_1}\frac{\partial A_2}{\partial \alpha_1} U_2\right], \tag{8}$$

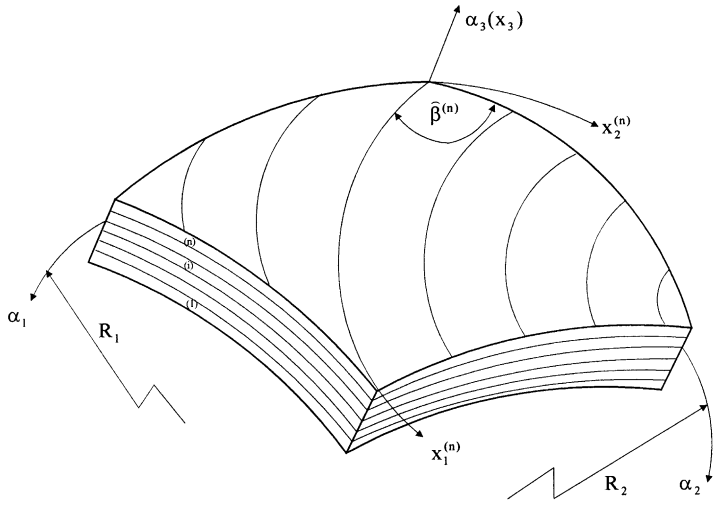


Figure 1. A piezo(electric)elastic laminated shell continuum.

$$S_{13} = \frac{1}{2(1 + \alpha_3/R_1)A_1}\left[\frac{\partial U_3}{\partial \alpha_1} - \frac{A_1}{R_1} U_1\right] + \frac{1}{2}\frac{\partial U_1}{\partial \alpha_3}, \tag{9}$$

$$S_{23} = \frac{1}{2(1 + \alpha_3/R_2)A_2}\left[\frac{\partial U_3}{\partial \alpha_2} - \frac{A_2}{R_2} U_2\right] + \frac{1}{2}\frac{\partial U_2}{\partial \alpha_3}, \tag{10}$$

$$E_1 = -\frac{1}{(1 + \alpha_3/R_1)A_1}\frac{\partial \phi}{\partial \alpha_1}, \quad E_2 = -\frac{1}{(1 + \alpha_3/R_2)A_2}\frac{\partial \phi}{\partial \alpha_2}, \quad E_3 = -\frac{\partial \phi}{\partial \alpha_3}, \tag{11}$$

where $S_{ij}$, $\phi$, and $E_i$ denote the strains, electric potential, and electric fields, respectively, $R_1$ and $R_2$ are the radii of principal curvature, and $A_1$ and $A_2$ are the Lamé parameters.

There are mechanical and electric boundary conditions associated with the piezoelastic shell continuum, i.e.,

$$U_i = \bar{U}_i, \qquad T_{ij}\ell_j = f_i, \tag{12, 13}$$

$$\phi = \bar{\phi}, \qquad D_i\ell_i = -Q, \tag{14, 15}$$

where $U_i$ is the displacement, $\ell_i$ is the direction cosine components, $f_i$ is the surface force, $\phi$ is the electric potential, $Q$ is the charge, and $(\bar{\cdot})$ denotes a known boundary value. Using the weighted residual method and introducing arbitrary weighting quantities $\delta U_i$ and $\delta\phi$, one can rewrite the weak form of the equilibrium equations as [17, 19]

$$\int_V \delta U_i(T_{ij,j} + f_{bi} - \rho\ddot{U}_i)\,\mathrm{d}V = 0, \qquad \int_V \delta\phi D_{i,i}\,\mathrm{d}V = 0, \tag{16, 17}$$

where the quantities $\delta U_i$ and $\delta\phi$ can be defined as the virtual displacement and electric potential respectively. Integrating each term by parts, taking into account of boundary

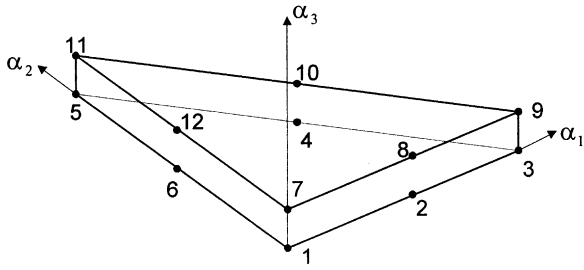


Figure 2. Triangular piezoelastic composite shell finite element.

conditions defined in equations (12)–(15), and noting that $\delta U_i = 0$ on $S_u$ and $\delta\phi = 0$ on $S_\phi$, one can simplify equations (16) and (17) to

$$\int_V T_{ij}\,\delta S_{ij}\,\mathrm{d}V - \int_{S_T} f_i\,\delta U_i\,\mathrm{d}S - \int_V (f_{bi} - \rho\ddot{U}_i)\,\delta U_i\,\mathrm{d}V = 0, \tag{18}$$

$$\int_V D_i \delta E_i\,\mathrm{d}V - \int_{S_D} Q\delta\phi\,\mathrm{d}S = 0, \tag{19}$$

Note that equations (18) and (19) are the virtual work expressions of the piezo(electric)-elastic shell continuum.

## 3. PIEZOELASTIC FINITE ELEMENT FORMULATION

A new 12-node, 48-degree-of-freedom curved triangular laminated piezoelastic shell element with *non-constant* radii of curvature (i.e., non-constant Lamé parameters) is developed. Figure 2 illustrates the triangular shell element and all its 12 nodes. Each node allows three displacement variables (i.e., $U_1^{(i)}(\gamma)$, $U_2^{(i)}(\gamma)$, and $U_3^{(i)}(\gamma)$) and one electric potential variable $\phi^{(i)}(\gamma)$ [14, 17].

Assumptions of layerwise constant shear angle and linear variation along the thickness of each layer are used in the finite element derivations. Thus, for an arbitrary $i$th layer, the displacements $U_1^{(i)}(\gamma)$, $U_2^{(i)}(\gamma)$, and $U_3^{(i)}(\gamma)$ and electric potential $\phi^{(i)}(\gamma)$ can be expressed as

$$U_1^{(i)}(\gamma) = \bar{U}_1^{(i)}\left(1 - \frac{\gamma}{h_i}\right) + \bar{U}_1^{(i+1)}\frac{\gamma}{h_i}, \quad U_2^{(i)}(\gamma) = \bar{U}_2^{(i)}\left(1 - \frac{\gamma}{h_i}\right) + \bar{U}_2^{(i+1)}\frac{\gamma}{h_i}, \tag{20, 21}$$

$$U_3^{(i)}(\gamma) = \bar{U}_3^{(i)}\left(1 - \frac{\gamma}{h_i}\right) + \bar{U}_3^{(i+1)}\frac{\gamma}{h_i}, \quad \phi^{(i)}(\gamma) = \bar{\phi}^{(i)}\left(1 - \frac{\gamma}{h_i}\right) + \bar{\phi}^{(i+1)}\frac{\gamma}{h_i}, \tag{22, 23}$$

where $\gamma$ is a transverse co-ordinate defined for the $i$th layer, $h_i$ is the thickness of the $i$th layer. The displacement and potential expressions can be simply written as functions of shape functions and the $i$th layer displacement vector

$$\{U^{(i)}(\gamma)\} = [N_u^{(i)}(\gamma)]\,\{\bar{U}^{(i)}\}, \qquad \phi^{(i)}(\gamma) = [N_\phi^{(i)}(\gamma)]\,\{\bar{\phi}^{(i)}\}, \tag{24, 25}$$

where $\{U^{(i)}(\gamma)\} = \{U_1^{(i)}(\gamma), U_2^{(i)}(\gamma), U_3^{(i)}(\gamma)\}^{\mathrm{t}}$ is a displacement vector of any point on the $i$th layer. $\{\bar{U}^{(i)}\} = \{\bar{U}_1^{(i)}, \bar{U}_2^{(i)}, \bar{U}_3^{(i)}, \bar{U}_1^{(i+1)}, \bar{U}_2^{(i+1)}, \bar{U}_3^{(i+1)}\}^{\mathrm{t}}$ and $\{\bar{\phi}^{(i)}\} = \{\bar{\phi}^{(i)}, \bar{\phi}^{(i+1)}\}^{\mathrm{t}}$ are the

displacements and electric potential of the $i$th and $(i+1)$th interfaces along the curvilinear co-ordinate axes. $[N_u^{(i)}(\gamma)]$ and $[N_\phi^{(i)}(\gamma)]$ are the shape functions in terms of the co-ordinate $\gamma$. The interpolation functions of the surface-parallel displacements and electric potential in each triangular region at the $i$th or $(i+1)$th interface are chosen to be continuous piecewise quadratic in the form

$$\begin{Bmatrix} \{\bar{U}^{(i)}\} \\ \{\bar{\phi}^{(i)}\} \end{Bmatrix} = a_1\alpha_1^2 + a_2\alpha_2^2 + a_3\alpha_1\alpha_2 + a_4\alpha_1 + a_5\alpha_2 + a_6, \tag{26}$$

where $a_i$ $(i = 1, \ldots, 6)$ are constants; and $\alpha_i (i = 1, 2, 3)$ are the global co-ordinates. Due to the continuity across the edge between two adjacent triangle elements, equation (40) becomes

$$\bar{U}_1^{(i)} = \{N\}^{\mathrm{t}}\{U_1^{(i)}\}, \qquad \bar{U}_2^{(i)} = \{N\}^{\mathrm{t}}\{U_2^{(i)}\}, \tag{27, 28}$$

$$\bar{U}_3^{(i)} = \{N\}^{\mathrm{t}}\{U_3^{(i)}\}, \qquad \bar{\phi}^{(i)} = \{N\}^{\mathrm{t}}\{\phi^{(i)}\}, \tag{29, 30}$$

where $\{U_1^{(i)}\} = \{U_{11}^i, \ldots, U_{16}^i\}^{\mathrm{t}}$, $\{U_2^{(i)}\} = \{U_{21}^i, \ldots, U_{26}^i\}^{\mathrm{t}}$, $\{U_3^{(i)}\} = \{U_{31}^i, \ldots, U_{36}^i\}^{\mathrm{t}}$ and $\{\phi^{(i)}\} = \{\phi_1^i, \ldots, \phi_6^i\}^{\mathrm{t}}$ are the nodal displacement and electric potential vectors of the element. $\{N\}$ is the quadratic shape function. Substituting equations (27)–(30) into equations (24) and (25) yields the following displacement $\{\bar{U}^{(i)}\}$ and electric potential $\{\bar{\phi}^{(i)}\}$ expressions:

$$\{\bar{U}^{(i)}\} = [N_{u_j}(\alpha_1, \alpha_2)]\{U_j^{(i)}\}, \qquad \{\bar{\phi}^{(i)}\} = [N_{\phi_j}(\alpha_1, \alpha_2)]\{\phi_j^{(i)}\}, \tag{31, 32}$$

where $\{U_j^{(i)}\} = \{U_{11}^i, U_{21}^i, U_{31}^i, \ldots, U_{16}^i, U_{26}^i, U_{36}^i, U_{11}^{i+1}, U_{21}^{i+1}, U_{31}^{i+1}, \ldots, U_{16}^{i+1}, U_{26}^{i+1}, U_{36}^{i+1}\}^{\mathrm{t}}$ and $\{\phi_j^{(i)}\} = \{\phi_1^i, \ldots, \phi_6^i, \phi_1^{i+1}, \ldots, \phi_6^{i+1}\}^{\mathrm{t}}$ are the nodal displacements and the nodal electric potential of the $j$th planar layer element located on the $i$th layer respectively. $[N_{u_j}(\alpha_1, \alpha_2)]$ and $[N_{\phi_j}(\alpha_1, \alpha_2)]$ are the shape functions of co-ordinates $\alpha_1$ and $\alpha_2$. Writing the shell strain–displacement and electric field–potential expressions in terms of nodal variables of the piezoelastic shell finite element gives

$$\begin{aligned} \{S^{(i)}(\gamma)\} &= [L_u^{(i)}][N_u^{(i)}(\gamma)][N_{u_j}(\alpha_1, \alpha_2)]\{U_j^{(i)}\} \\ &= [B_u^{(i)}(\gamma)][B_{u_j}(\alpha_1, \alpha_2)]\{U_j^{(i)}\}, \end{aligned} \tag{33}$$

$$\begin{aligned} \{E^{(i)}(\gamma)\} &= -[L_\phi^{(i)}][N_\phi^{(i)}(\gamma)][N_{\phi_j}(\alpha_1, \alpha_2)]\{\phi_j^{(i)}\} \\ &= -[B_\phi^{(i)}(\gamma)][B_{\phi_j}(\alpha_1, \alpha_2)]\{\phi_j^{(i)}\}, \end{aligned} \tag{34}$$

Substituting the constitutive equations (1) and (2), displacement-shape function equations (24) and (25) and (31)–(34) into the equilibrium equations (18) and (19), one can derive the nodal governing equations of the $j$th (planar) element located on the $i$th (thickness) layer in matrix form,

$$\begin{bmatrix} [M_{uu_j}^{(i)}] & 0 \\ 0 & 0 \end{bmatrix} \begin{Bmatrix} \{\ddot{U}_j^{(i)}\} \\ \{\ddot{\phi}_j^{(i)}\} \end{Bmatrix} + \begin{bmatrix} [C_{uu_j}^{(i)}] & 0 \\ 0 & 0 \end{bmatrix} \begin{Bmatrix} \{\dot{U}_j^{(i)}\} \\ \{\dot{\phi}_j^{(i)}\} \end{Bmatrix}$$

$$+ \begin{bmatrix} [K_{uu_j}^{(i)}] & [K_{u\phi_j}^{(i)}] \\ [K_{\phi u_j}^{(i)}] & [K_{\phi\phi_j}^{(i)}] \end{bmatrix} \begin{Bmatrix} \{U_j^{(i)}\} \\ \{\phi_j^{(i)}\} \end{Bmatrix} = \begin{Bmatrix} \{F_{u_j}^{(i)}\} \\ \{F_{\phi_j}^{(i)}\} \end{Bmatrix}, \tag{35}$$

where $[M^{(i)}_{uu_j}]$ is the mass matrix, $[C^{(i)}_{uu_j}]$ is the damping matrix, $[K^{(i)}_{xy_j}]$ (where $x$ and $y = u, \phi$), are the stiffness matrices defined for the displacement and electric potential, and $\{F^{(i)}_{u_j}\}$ and $\{F^{(i)}_{\phi_j}\}$ are the mechanical and electric excitations. Detailed element matrices of a laminated piezoelastic shell element are presented in Appendix A. The element damping matrix $[C^{(i)}_{uu_j}]$ is assumed to be proportional to the stiffness and mass matrices: $[C^{(i)}_{uu_j}] = \alpha[M^{(i)}_{uu_j}] + \beta[K^{(i)}_{uu_j}]$, where $\alpha$ and $\beta$ are Rayleigh's coefficients and are related to $\alpha + \beta\omega_i^2 = 2\xi_i\omega_i$, and $\xi_i$ and $\omega_i$ are the initial damping ratio and natural frequencies [17]. If two damping ratios and two natural frequencies are specified, the damping estimation results in an exact solution for $\alpha$ and $\beta$. If more than two damping ratios and frequencies are specified, a least-squares solution procedure can be used to determine $\alpha$ and $\beta$. Assembling all element matrices yields the global system matrix equation

$$\begin{bmatrix} [M_{uu}] & 0 \\ 0 & 0 \end{bmatrix} \begin{Bmatrix} \{\ddot{U}\} \\ \{\ddot{\phi}\} \end{Bmatrix} + \begin{bmatrix} [C_{uu}] & 0 \\ 0 & 0 \end{bmatrix} \begin{Bmatrix} \{\dot{U}\} \\ \{\dot{\phi}\} \end{Bmatrix} + \begin{bmatrix} [K_{uu}] & [K^{(i)}_{u\phi}] \\ [K_{\phi u}] & [K_{\phi\phi}] \end{bmatrix} \begin{Bmatrix} \{U\} \\ \{\phi\} \end{Bmatrix} = \begin{Bmatrix} \{F_u\} \\ \{F_\phi\} \end{Bmatrix}. \quad (36)$$

For static applications, the dynamic system equation is reduced to

$$\begin{bmatrix} [K_{uu}] & [K_{u\phi}] \\ [K_{\phi u}] & [K_{\phi\phi}] \end{bmatrix} \begin{Bmatrix} \{U\} \\ \{\phi\} \end{Bmatrix} = \begin{Bmatrix} \{F_u\} \\ \{F_\phi\} \end{Bmatrix}. \quad (37)$$

In constant-gain negative velocity feedback control, the feedback control forces $\{F^a_f\}$ are given by [5]

$$\{F^a_f\} = -[K_{u\phi}][K_{\phi\phi}]^{-1} G C_p [K_{\phi\phi}]^{-1} [K_{\phi u}]\{\dot{U}\}, \quad (38)$$

where $G$ is the gain, $C_p$ is the actuator capacitance, $[\cdot]^{-1}$ denotes the matrix inverse, and $\{\dot{U}\}$ is the velocity. Note that, in this case, the feedback gain is constant while the feedback amplitude varies with respect to the negative oscillating velocity (*negative velocity*, *constant gain proportional feedback control*) [5, 16, 17]. The developed new piezoelastic shell element with non-constant Lamé parameters and the finite element code are used to investigate the dynamics and the distributed control of conical shells is presented next.

## 4. DYNAMICS AND CONTROL OF CONICAL SHELLS

Conical shells are widely used as parts or components of nozzles, rocket fairings, etc., in aerospace structures and turbomachinery. The dynamics and distributed control of conical shells and other shells of revolution with non-constant Lamé parameters can be studied based on the new piezoelastic shell element with non-constant radii of curvature. A conical shell panel laminated with distributed piezoelectric layers is clamped at one end and free on the other three edges (i.e., CFFF). The conical shell is defined in Figure 3 and its dimensions are shown in Figure 4. Geometry and material properties are provided in Table 1. Natural frequencies and modes of a conical shell panel are investigated first and finite element solutions are compared with published numerical results. Distributed vibration control of conical shells with (1) the fully distributed piezoelectric actuator, (2) the partial-diagonally distributed actuator, and (3) the full-diagonally distributed actuator are investigated and their control effects are evaluated in this section.

The conical shell panel is divided into $(20 \times 10)$ meshes along the longitudinal and circumferential directions respectively. Therefore, there are 400 triangular shell elements for each layer and total 1200 elements are used for the panel, Figure 5.

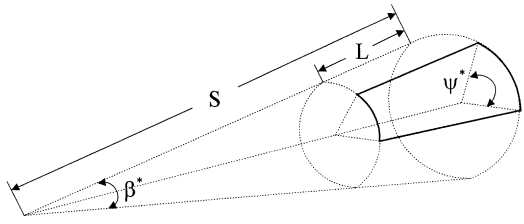


Figure 3. A conical shell panel and its co-ordinate system.

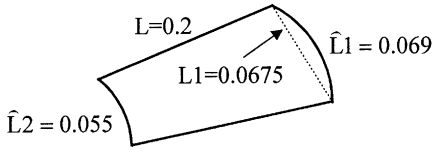


Figure 4. Dimensions of the conical shell panel.

TABLE 1

*Geometry and material properties of the laminated conical shell*

| | Aluminum | PVDF |
|---|---|---|
| Length, $S$ (m) | 1·0 | |
| Length, $L$ (m) | 0·2 | |
| Semi-vertex angle, $\beta^*$ (°) | 15 | |
| Meridional angle, $\psi^*$ (°) | 30·247 | |
| Thickness, $h$ (m) | $1 \times 10^{-3}$ | $9 \times 10^{-6}$ |
| Density, $\rho$ (Kg/m$^3$) | $2{\cdot}6573 \times 10^3$ | $1{\cdot}8 \times 10^3$ |
| Young's modulus, $Y$ (Pa) | $6{\cdot}8947 \times 10^{10}$ | $2{\cdot}0 \times 10^9$ |
| The Poisson constant, $\mu$ | 0·3 | 0·29 |
| Piezostrain constant, $d_{31}$ (m/V) | | $2{\cdot}2 \times 10^{-11}$ |
| Electric permittivity, $\varepsilon_{11}$ (F/m) | | $1{\cdot}062 \times 10^{-10}$ |
| Capacitance, $C$ (F/m$^2$) | | $3{\cdot}80 \times 10^{-6}$ |

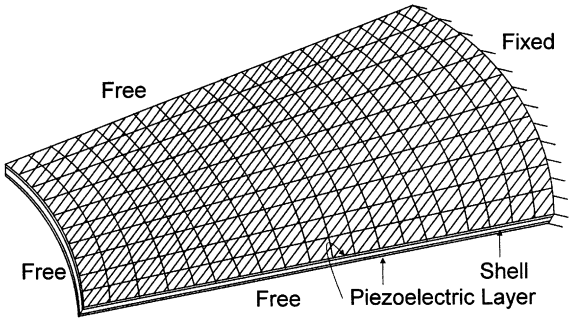


Figure 5. Finite element model of the conical shell panel laminated with fully distributed piezoelectric layers.

### 4.1. FREE VIBRATION ANALYSIS

Natural frequencies and mode shapes of the conical shell panel are studied first. In order to compare with published data, the dimensionless frequency parameter

TABLE 2

*Comparison of FE solutions with published data*

| Source | $\lambda_1$ | $\lambda_2$ | $\lambda_3$ | $\lambda_4$ | $\lambda_5$ | $\lambda_6$ | $\lambda_7$ | $\lambda_8$ |
|---|---|---|---|---|---|---|---|---|
| FE | 5·3182 | 8·7357 | 27·300 | 28·973 | 51·111 | 65·595 | 72·416 | 81·477 |
| [1] | 5·5130 | 8·9563 | 26·989 | 28·852 | 50·174 | 64·497 | 75·479 | 79·578 |
| [1] | 5·5179 | 8·9608 | 27·014 | 28·909 | 50·267 | 64·631 | 75·541 | 79·815 |
| [2] | 6·1727 | 9·0708 | 27·299 | 29·758 | 50·669 | 65·171 | 74·499 | 80·201 |

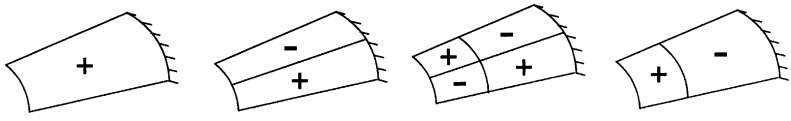


Figure 6. The first four mode shapes of the conical shell panel.

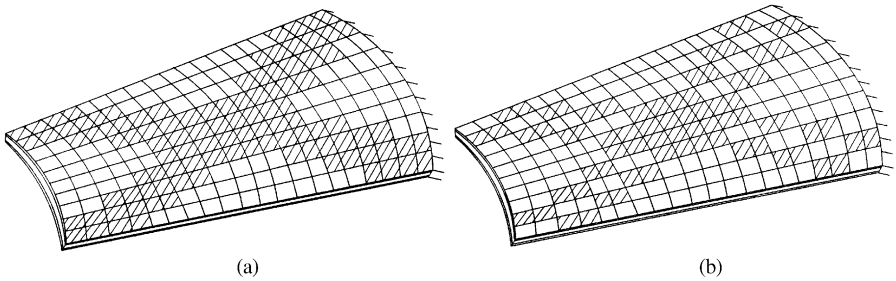


Figure 7. Conical shell panel with (a) full- and (b) partial-diagonally laminated actuators.

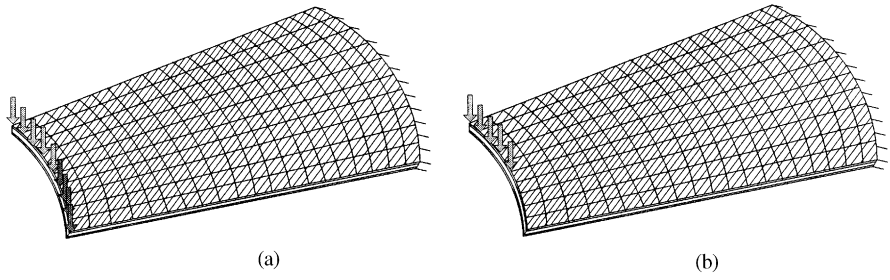


Figure 8. Two loading conditions: (a) full-edge loading, (b) half-edge loading.

$\lambda_n = \omega_n(\beta^*, \psi^*)LL_1(\rho h/D)^{1/2}$ is used where $\omega_n$ is the circular frequency, $\rho$ is the mass density, $L$ is the length of the conical shell panel in the longitudinal direction, $L_1$ is the projected length of the major edge shown in Figure 4, $h$ is the shell thickness and $D$ is the bending stiffness coefficient $D = (Yh^3)/[12(1 - \mu^2)]$. Finite element solutions (FE) are compared with published numerical results [1, 2] in Table 2.

These data and comparison suggest that the developed finite element code is capable of analyzing conical shells accurately. The first four mode shapes of the conical shell panel are calculated and they are illustrated in Figure 6.

### 4.2. DISTRIBUTED VIBRATION CONTROL

The conical shell panel is laminated with two piezoelectric layers on the top and bottom surfaces serving as sensor and actuator respectively. Three actuator lamination configurations: the full lamination (Figure 5), the partial-diagonal lamination and the full-diagonal lamination (Figure 7) are designed to evaluate their control effectiveness. Two uniform transverse line loadings with a sum of 1 N are applied on the minor-radius free edge. One is applied on the whole free-end edge and the other is applied only on half of the free end, Figure 8. In general, the initial loading is applied to the free edge first. Then the shell is released and free to oscillate. Free oscillation responses of the conical shells with and without distributed control are evaluated and their inferred damping ratios with different control gains (0, 10, 20, 25) for three lamination configurations are evaluated. Note that control signals generated from the control gains are within the breakdown voltage of the distributed piezoelectric actuators.

### 4.3. CASE 1: FULL-EDGE LOADING

Time histories of the free and controlled responses of the conical shell at the *full-edge loading* are plotted in Figures 9–13 and inferred damping ratios are summarized in

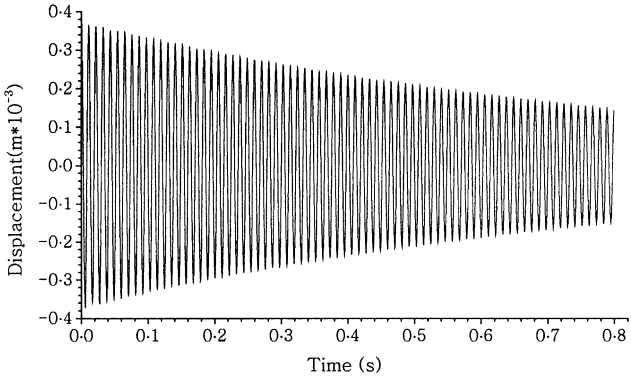


Figure 9. Free displacement response (full-edge loading).

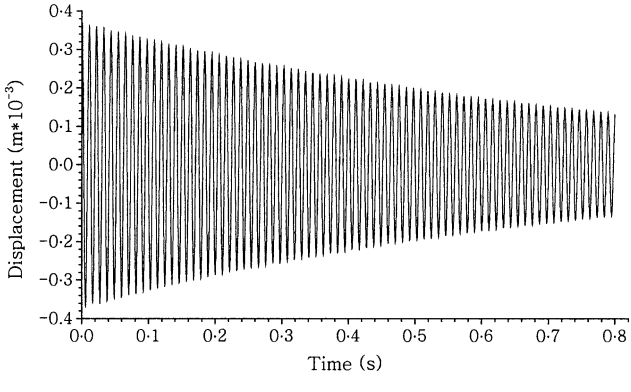


Figure 10. Controlled response (gain = 25) (fully distributed actuator).

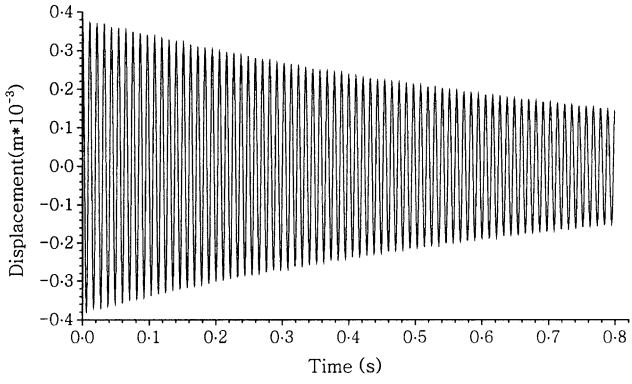


Figure 11. Controlled response (gain = 25) (partial-diagonal actuator).

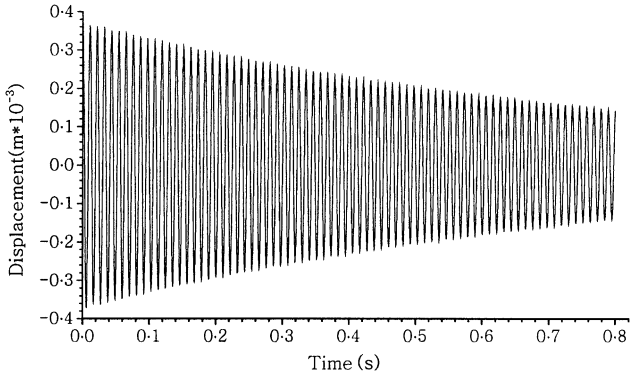


Figure 12. Controlled response (gain = 25) (full-diagonal actuator).

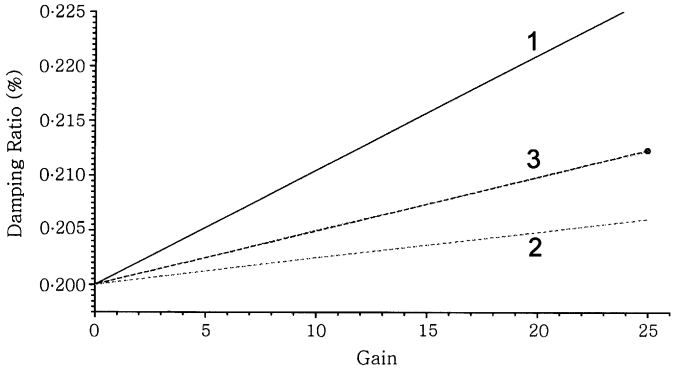


Figure 13. Inferred damping ratios at different gains (full-edge loading): 1, full lamination; 2, partial-diagonal lamination; 3, full-diagonal lamination.

Figure 13. Note that Figure 9 is the free response, Figure 10 is the controlled response with the fully distributed actuator, Figure 11 is the controlled response with the partial-diagonal actuator, and Figure 12 is the controlled response with the full-diagonal actuator. In general, the first-mode response dominates both the free and controlled responses. Note that all controlled responses were based on the negative velocity constant-gain feedback control algorithm.

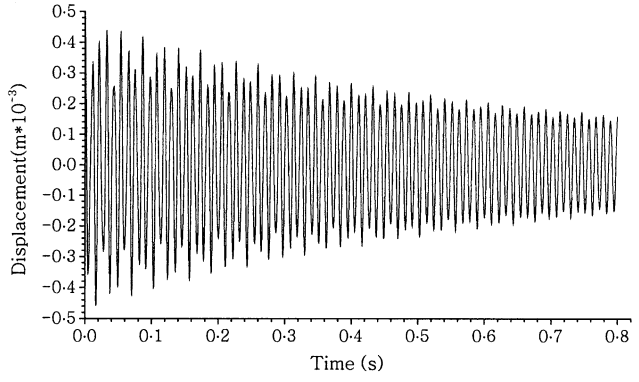


Figure 14. Free displacement response (half-edge loading).

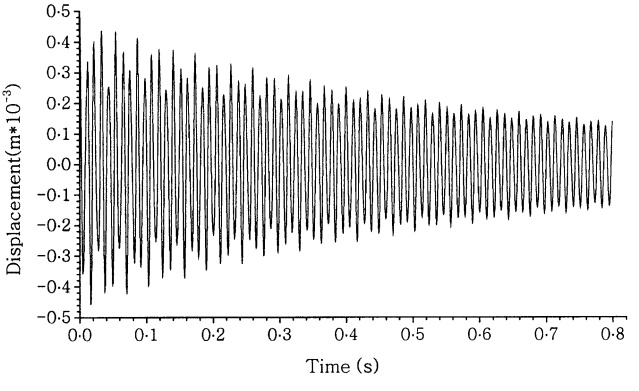


Figure 15. Controlled response (gain = 25) (fully distributed actuator).

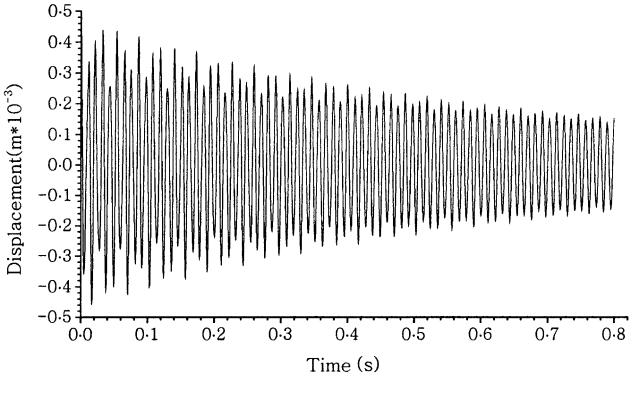


Figure 16. Controlled response (gain = 25) (partial-diagonal actuator).

## 4.4. CASE 2: HALF-EDGE LOADING

Again, time histories of the free and controlled responses of the conical shell at the *half-edge loading* are plotted in Figures 14–17 and inferred damping ratios are summarized

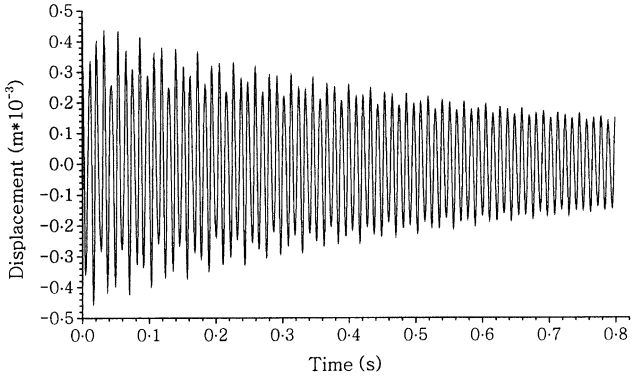


Figure 17. Controlled response (gain = 25) (full-diagonal actuator).

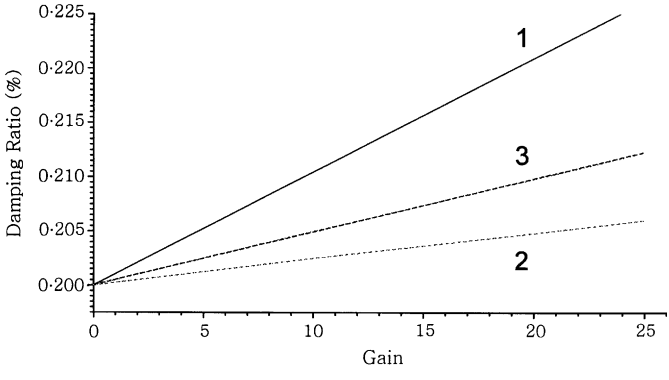


Figure 18. Inferred damping ratios at different gains (half-edge loading). 1, full lamination; 2, partial-daigonal lamination; 3, full-diagonal lamination.

in Figure 18. All time-history responses reveal both the first-mode and higher mode frequency components, due to unsymmetrical half-edge loading.

These free and controlled time-history responses reveal that the responses are absolutely dominated by the first-mode at the full-edge loading, while higher mode components appear in the responses at the half-edge loading. On the three actuator configurations, the full-lamination configuration has the best control effect and the partial-diagonal lamination configuration has the least control effect for the first-mode oscillation. The fully distributed actuator configuration is effective for the bending dominated natural modes, e.g., the first mode and the fourth mode, Figure 6. The two diagonally laminated actuator configurations would have better control effects for second-mode and third-mode oscillations, since torsion behaviors appear in these two modes [20].

## 5. SUMMARY AND CONCLUSION

Full or partial conical shells often appear as nozzles, injectors, blades, rocket fairings, etc., in aerospace structures and turbomachinery. Undesirable dynamic oscillations not only degrade the performance, but also influence structural integrity and reliability. This report is to evaluate dynamic characteristics and control effectiveness of conical shells laminated with distributed piezoelectric sensor/actuator layers.

Electromechanical constitutive equations, governing equations, strain–displacement–electric field relations, and boundary conditions of a generic piezo(electric)elastic shell continuum were presented first. Finite element formulations of a new triangular piezoelastic shell element with non-constant Lamé parameters were presented, electromechanical element/system/control matrix equations were derived, and then control algorithms defined. Finite element models of a conical shell with three actuator lamination configurations (i.e., the fully distributed, the partial-diagonally distributed, and the full-diagonally distributed) were established and two loading conditions (i.e., the full-edge loading and the half-edge loading) were defined, too.

Natural frequencies and modes of the conical shell finite element models were calculated using the newly developed finite element code. Finite element solutions were compared closely with published numerical results. Thus, the newly developed tool is effective in modelling and analysis of conical shells. Free and controlled time-history responses of the two loading conditions were studied and inferred damping ratios suggest that the fully-distributed configuration is effective in the control of bending-dominated natural modes, e.g., first and fourth modes; the diagonally laminated configurations are effective in the control of torsion-dominated modes, e.g., second and third modes in this case. Accordingly, distributed control of conical shells can be achieved. However, this study suggests that various actuator configurations contribute to a difference in control effectiveness for the various natural modes. To maximize the distributed control effects, an in-depth understanding of shell dynamics and dominating modes is a must in the effective design and layout of distributed actuators.

## ACKNOWLEDGMENTS

This research is supported, in part, by a grant (F49620-98-1-0467) from the Air Force Office of Scientific Research (Project Manager: Brian Sanders). This support is gratefully acknowledged.

## REFERENCES

1. N. S. Bardell 1998 *Journal of Sound and Vibration* **217**, 297–320. Free vibration of thin, isotropic, open conical panels.
2. C. W. Lim and K. M. Liew 1995 *Engineering Structures* **17**, 63–70. Vibratory behavior of shallow conical shells by a global Ritz formulation.
3. U. Gabbert and H. S. Tzou 2001 *Smart Structures and Structronic Systems*. Boston/Dordrecht: Kluwer Academic Publishers.
4. H. S. Tzou and G. L. Anderson 1992 *Intelligent Structural Systems*. Boston/Dordrecht: Kluwer Academic Publishers.
5. H. S. Tzou 1993 *Piezoelectric Shells* (*Distributed Sensing and Control of Continua*). Boston/Dordrecht: Kluwer Academic Publishers.
6. A. Baz and S. Poh 1988 *Journal of Sound and Vibration* **126**, 327–343. Performance of an active control system with piezoelectric actuators.
7. E. F. Crawley and K. B. Lazarus 1991 *American Institute of Aeronautics and Astronautics Journal* **29**, 944–951. Induced strain actuation of isotropic and anisotropic plates.
8. J. E. Hubbard and S. E. Burke 1992 in *Intelligent Structural Systems* (H. S. Tzou and G. L. Anderson, editors), 305–324. Boston/Dordrecht: Kluwer Academic Publishers. Distributed transducer design for intelligent structural components.
9. S. K. Ha, C. Keilers and F. K. Chang 1992 *American Institute of Aeronautics and Astronautics Journal* **30**, 772–780. Finite element analysis of composite structures containing distributed piezoceramics sensors and actuators.

10. C. K. LEE 1992 in *Intelligent Structural Systems* (H. S. Tzou and G. L. Anderson, editors), 75–167. Boston/Dordrecht: Kluwer Academic Publishers. Piezoelectric laminates: theory and experimentation for distributed sensors and actuators.
11. Y. GU, R. L. CLARK, C. R. FULLER and A. C. ZANDER 1994 *American Society of Mechanical Engineers Journal of Vibration and Acoustics* **116**, 303–308. Experiments on active control of plate vibration using piezoelectric actuators and polyvinylidene fluoride modal sensors.
12. H. S. TZOU, Y. BAO, and V. B. VENKAYYA 1996 *Journal of Sound and Vibration* **197**, 207–249. Study of segmented transducers laminated on cylindrical shells, part-1: sensor patches and part-2: actuator patches.
13. Y. H. ZHOU and H. S. TZOU 2000 *Journal of Solids and Structures* **37**, 1663–1677. Control of nonlinear piezoelectric circular shallow spherical shells.
14. H. S. TZOU and R. YE 1996 *American Institute of Aeronautics and Astronautics Journal* **34**, 110–115. Analysis of piezoelastic structures with laminated piezoelectric triangle shell elements.
15. H. S. TZOU and R. V. HOWARD 1994 *American Society of Mechanical Engineers, Journal of Vibration and Acoustics* **116**, 295–302. A piezothermoelastic shell theory applied to active structures.
16. H. S. TZOU and R. YE 1994 *American Society of Mechanical Engineers, Journal of Vibration and Acoustics* **114**, 489–495. Piezothermoelasticity and precision control of active piezoelectric laminates.
17. H. S. TZOU and R. YE 2000 *Journal of Sound and Vibration* **231**, 1321–1338. Control of adaptive shells with thermal and mechanical excitations,
18. R. D. MINDLIN 1961 in *Problems on Continuum Mechanics* (J. Radok, editor), *Society of Industrial and Applied Mathematics, Philadelphia*, 282–290. On the equations of motion of piezoelectric crystals.
19. O. C. ZIENKIEWICZ and R. L. TAYLOR 1989 *The Finite Element Method*. Vol. 1. New York: McGraw-Hill; fourth edition. Basic formulation and linear problems.
20. H. S. TZOU, R. YE and J. H. DING 2001 *Journal of Sound and Vibration* **241**, 271–281. A new X-actuator design for controlling wing bending and twisting modes.

## APPENDIX A: FORMULATION OF ELEMENT MATRICES

Detailed element matrices of a laminated piezoelastic shell element are presented here

$$[M_{uu_j}^{(i)}] = \int_{S_j} [N_{u_j}(\alpha_1, \alpha_2)]^{\mathrm{t}} \left( \int_{\gamma=0}^{h_i} [N_u^{(i)}(\gamma)]^{\mathrm{t}} \rho^{(i)} [N_u^{(i)}(\gamma)] B_1^i B_2^i \, \mathrm{d}\gamma \right) \times [N_{u_j}(\alpha_1, \alpha_2)] A_1 A_2 \, \mathrm{d}\alpha_1 \, \mathrm{d}\alpha_2, \tag{A.1}$$

$$[K_{uu_j}^{(i)}] = \int_{S_j} [B_{u_j}(\alpha_1, \alpha_2)]^{\mathrm{t}} \left( \int_{\gamma=0}^{h_i} [B_u^{(i)}(\gamma)]^{\mathrm{t}} [\bar{c}^{(i)}] [B_u^{(i)}(\gamma)] B_1^i B_2^i \, \mathrm{d}\gamma \right) \times [B_{u_j}(\alpha_1, \alpha_2)] A_1 A_2 \, \mathrm{d}\alpha_1 \, \mathrm{d}\alpha_2, \tag{A.2}$$

$$[K_{u\phi_j}^{(i)}] = \int_{S_j} [B_{u_j}(\alpha_1, \alpha_2)]^{\mathrm{t}} \left( \int_{\gamma=0}^{h_i} [B_u^{(i)}(\gamma)]^{\mathrm{t}} [\bar{e}^{(i)}] [B_\phi^{(i)}(\gamma)] B_1^i B_2^i \, \mathrm{d}\gamma \right) \times [B_{\phi_j}(\alpha_1, \alpha_2)] A_1 A_2 \, \mathrm{d}\alpha_1 \, \mathrm{d}\alpha_2, \tag{A.3}$$

$$[K_{\phi\phi_j}^{(i)}] = -\int_{S_j} [B_{\phi_j}(\alpha_1, \alpha_2)]^{\mathrm{t}} \left( \int_{\gamma=0}^{h_i} [B_\phi^{(i)}(\gamma)]^{\mathrm{t}} [\bar{\varepsilon}^{(i)}] [B_\phi^{(i)}(\gamma)] B_1^i B_2^i \, \mathrm{d}\gamma \right) \times [B_{\phi_j}(\alpha_1, \alpha_2)] A_1 A_2 \, \mathrm{d}\alpha_1 \, \mathrm{d}\alpha_2, \tag{A.4}$$

$$[K_{\phi u_j}^{(i)}] = [K_{\phi u_j}^{(i)}]^{\mathrm{t}}, \tag{A.5}$$

$$\{F_{u_j}^{(i)}\} = \int_{S_j} [N_{u_j}(\alpha_1, \alpha_2)]^{\mathrm{t}} [N_u^{(i)}(\gamma = h_x)]^{\mathrm{t}} \{f^{(i)}\} B_1^i(\gamma = h_x) B_2^i(\gamma = h_x) A_1 A_2 \, \mathrm{d}\alpha_1 \, \mathrm{d}\alpha_2$$

$$+ \int_{S_j} [N_{u_j}(\alpha_1, \alpha_2)]^{\mathrm{t}} \left( \int_{\gamma=0}^{h_i} [N_u^{(i)}(\gamma)]^{\mathrm{t}} \{f_b^{(i)}\} B_1^i B_2^i \, \mathrm{d}\gamma \right) A_1 A_2 \, \mathrm{d}\alpha_1 \, \mathrm{d}\alpha_2, \tag{A.6}$$

$$\{F_{\phi_j}^{(i)}\} = - \int_{S_j} [N_{\phi_j}(\alpha_1, \alpha_2)]^{\mathrm{t}} [N_\phi^{(i)}(\gamma = h_x)]^{\mathrm{t}} Q^i B_1^i(\gamma = h_x) B_2^i(\gamma = h_x) A_1 A_2 \, \mathrm{d}\alpha_1 \, \mathrm{d}\alpha_2. \tag{A.7}$$

where $\{f^{(i)}\} = \{f_1^{(i)}, f_2^{(i)}, f_3^{(i)}\}^{\mathrm{t}}$ and $\{f_b^{(i)}\} = \{f_{b1}^{(i)}, f_{b2}^{(i)}, f_{b3}^{(i)}\}^{\mathrm{t}}$ are the surface force and body force along the curvilinear co-ordinate axes, respectively, $Q^i$ is the electric charge applied on the surfaces of piezoelectric layers; and the thickness $0{\cdot}0 \leqslant h_x \leqslant h_i$.